

Measurement of Nucleon Strange Form Factors at High Q^2

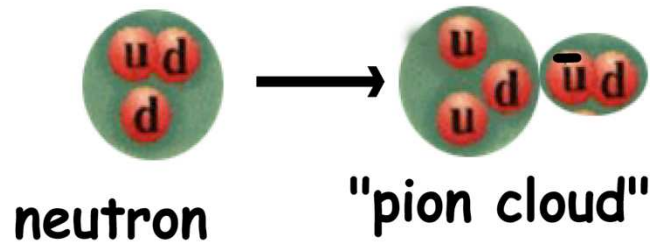
(HAPPEX III Collaboration)

Rupesh Silwal

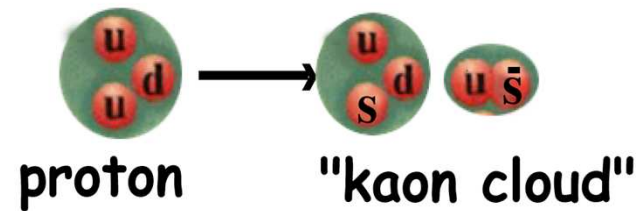
22 March, 2011

At very low Q^2 , G_E/M relates to the strange matrix elements of the nucleon (strange radius r_s and strange magnetic moment μ_s)

neutron charge distribution



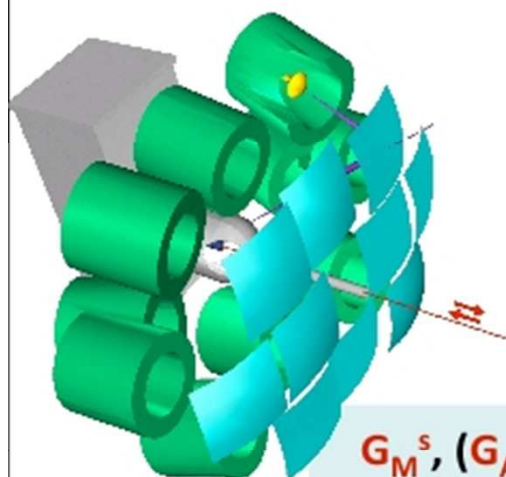
proton flavor distribution



The bare mass of the three valence quarks only makes up $\sim 1\%$ of the proton mass, the rest is a sea of gluons, quarks and anti-quarks, which is dominated by the up, down and strange quarks.

Do the strange quarks contribute to the electric and magnetic structure of the proton?

World Data



SAMPLE

open geometry,
integrating

$$G_M^s, (G_A) \text{ at } Q^2 = 0.1 \text{ GeV}^2$$

A4

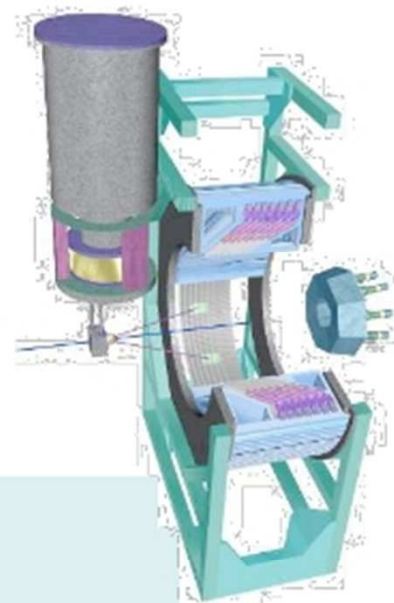
Open geometry

Fast counting calorimeter for
background rejection

$$G_E^s + 0.23 G_M^s \text{ at } Q^2 = 0.23 \text{ GeV}^2$$

$$G_E^s + 0.10 G_M^s \text{ at } Q^2 = 0.1 \text{ GeV}^2$$

$$G_M^s, G_A^e \text{ at } Q^2 = 0.23 \text{ GeV}^2$$



HAPPEX

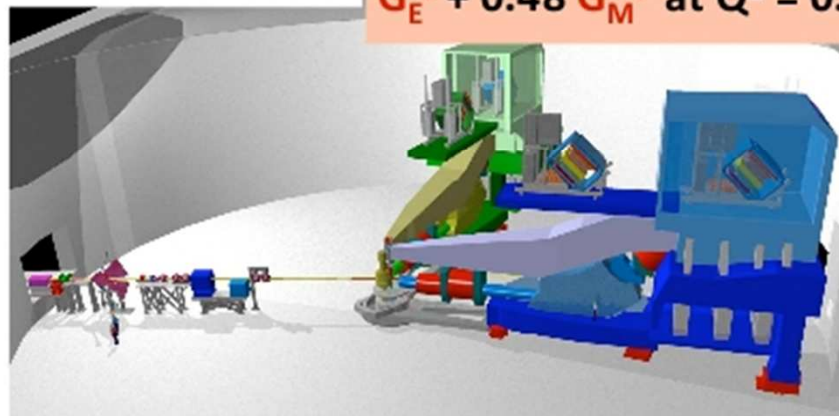
Precision
spectrometer,
integrating

$$G_E^s + 0.39 G_M^s \text{ at } Q^2 = 0.48 \text{ GeV}^2$$

$$G_E^s + 0.08 G_M^s \text{ at } Q^2 = 0.1 \text{ GeV}^2$$

$$G_E^s \text{ at } Q^2 = 0.1 \text{ GeV}^2 \text{ } (^4\text{He})$$

$$G_E^s + 0.48 G_M^s \text{ at } Q^2 = 0.62 \text{ GeV}^2$$



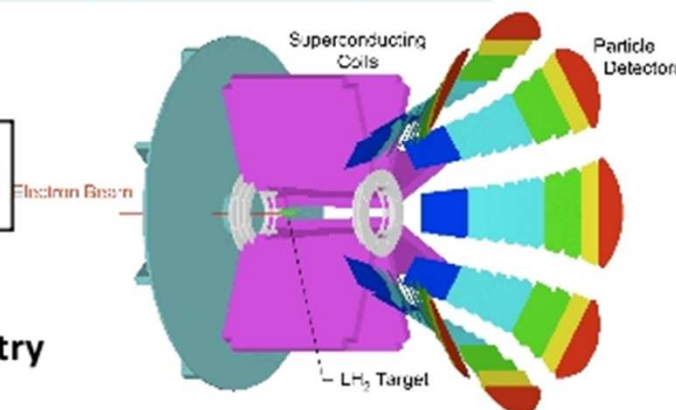
G0

Open geometry

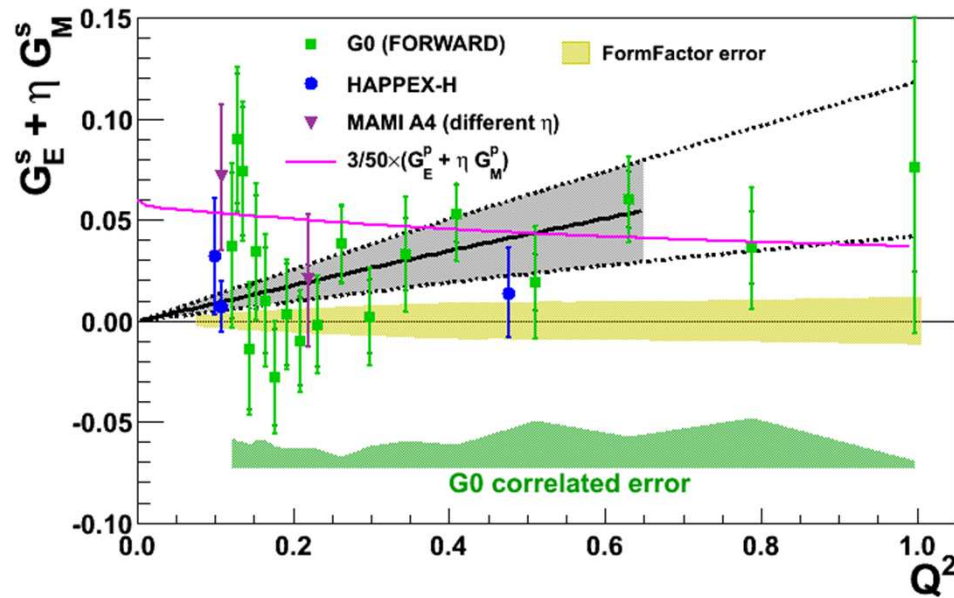
Fast counting with magnetic spectrometer + timing for
background rejection

$$G_E^s + \eta G_M^s \text{ over } Q^2 = [0.12, 1.0] \text{ GeV}^2$$

$$G_M^s, G_A^e \text{ at } Q^2 = 0.23, 0.62 \text{ GeV}^2$$



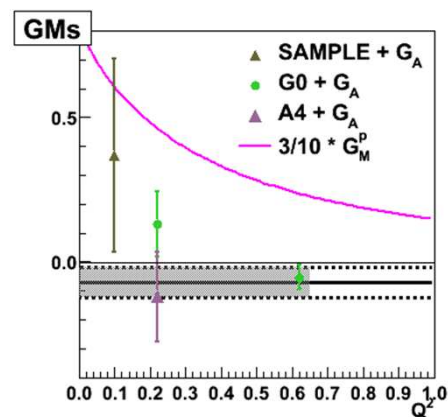
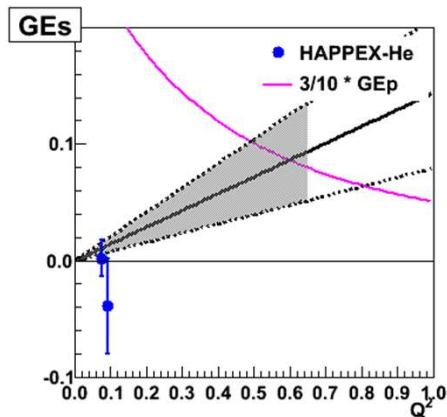
Present Data



Fit to “leading order” in Q^2 ,
 (only for $Q^2 < 0.65 \text{ (GeV/c)}^2$)

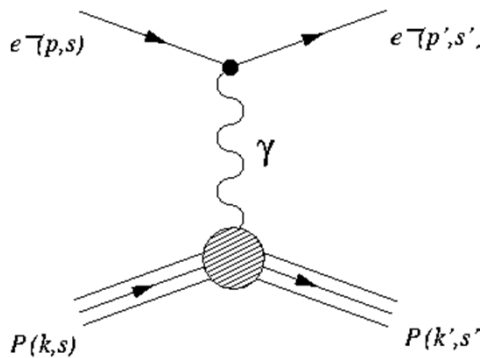
$$G_M^s = \mu_s$$

$$G_E^s = \rho_s * \tau$$

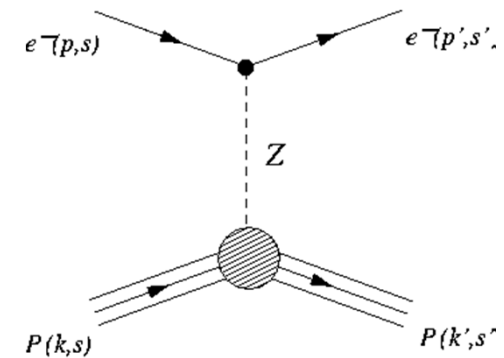


G_M^s From backangle
 results, neglects
 correlation with G_E^s

Parity-Violation



	Left	Right
Z-Charge	$\frac{1}{2} - q \sin^2 \theta$	$q \sin^2 \theta$



$$\sigma = |A_\gamma + AZ_0|^2$$

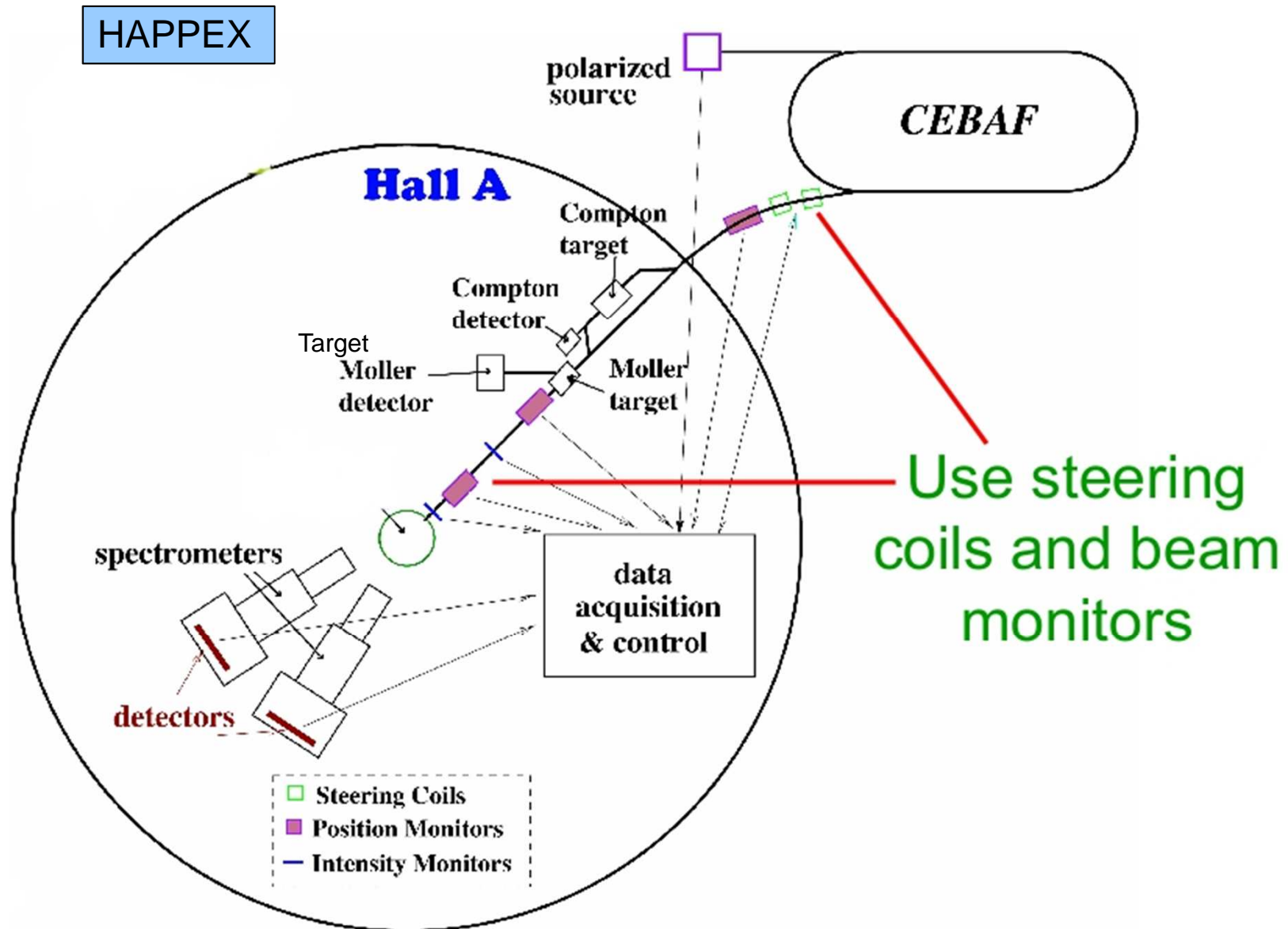
$$\sim |A_\gamma|^2 + 2A_\gamma A_{Z_0}^* + \dots$$

Left/Right handed longitudinally polarized electrons have different cross sections, which can vary by as much as 0.1%.

Weak Amplitude is 10^{-6} smaller than the Electromagnetic Amplitude, but its interference to EM makes it accessible.

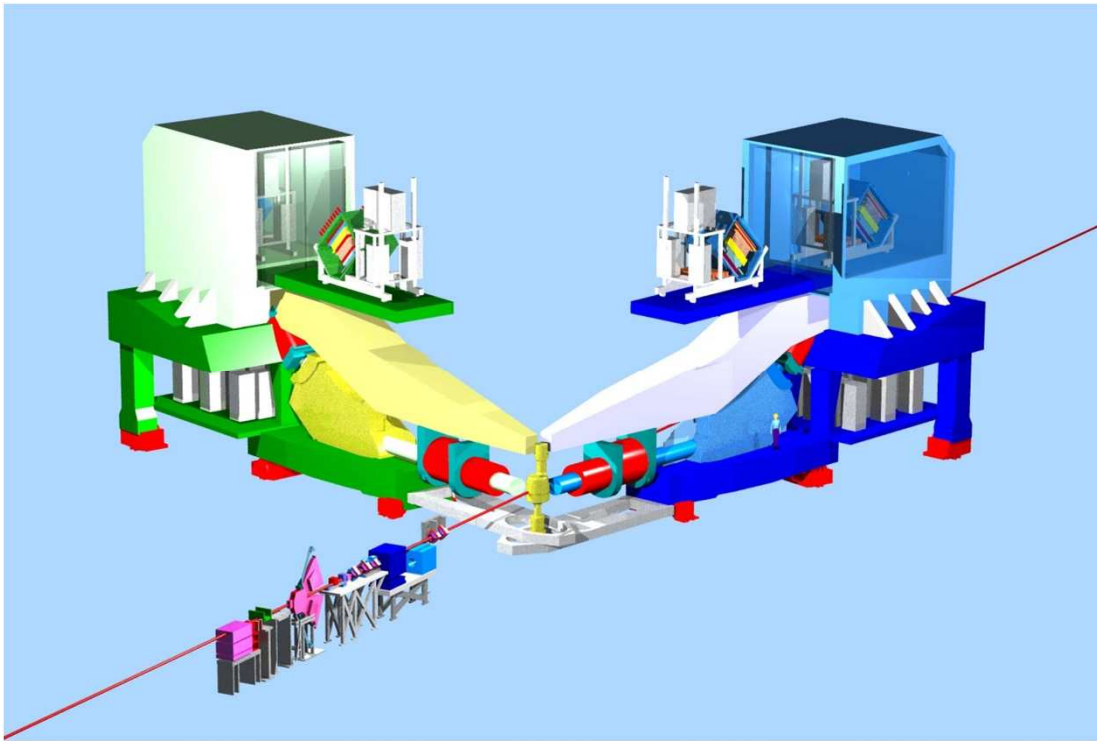
$$A_{PV} = \frac{\sigma_R - \sigma_L}{\sigma_R + \sigma_L} \sim \frac{\langle \gamma \rangle \langle Z^0 \rangle}{|\langle \gamma \rangle|^2} \sim \frac{A_\gamma}{A_{Z_0}}$$

Experimental Setup

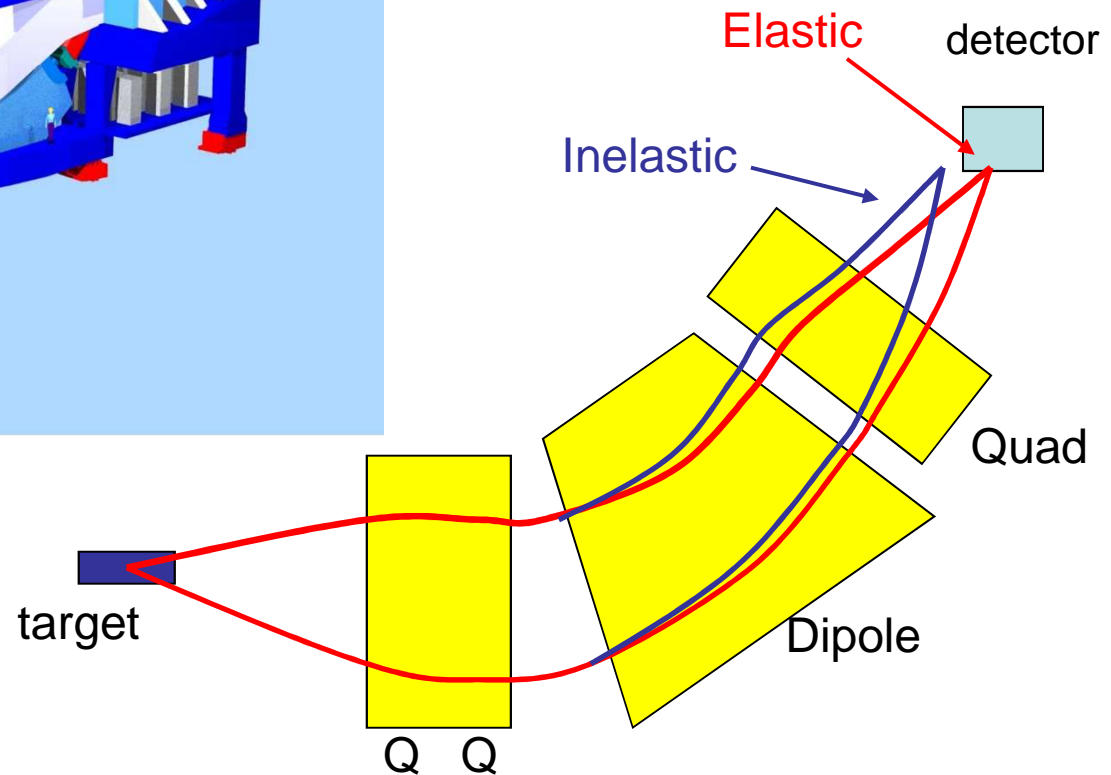


High Resolution Spectrometers

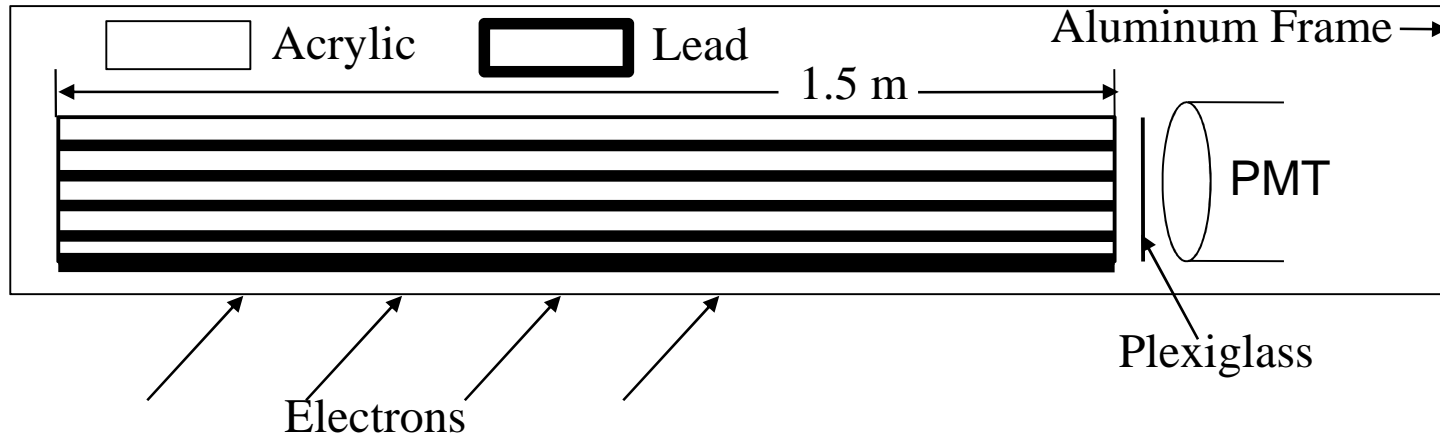
Spectrometer Concept:
Resolve Elastic



Left-Right symmetry to
control transverse
polarization systematic

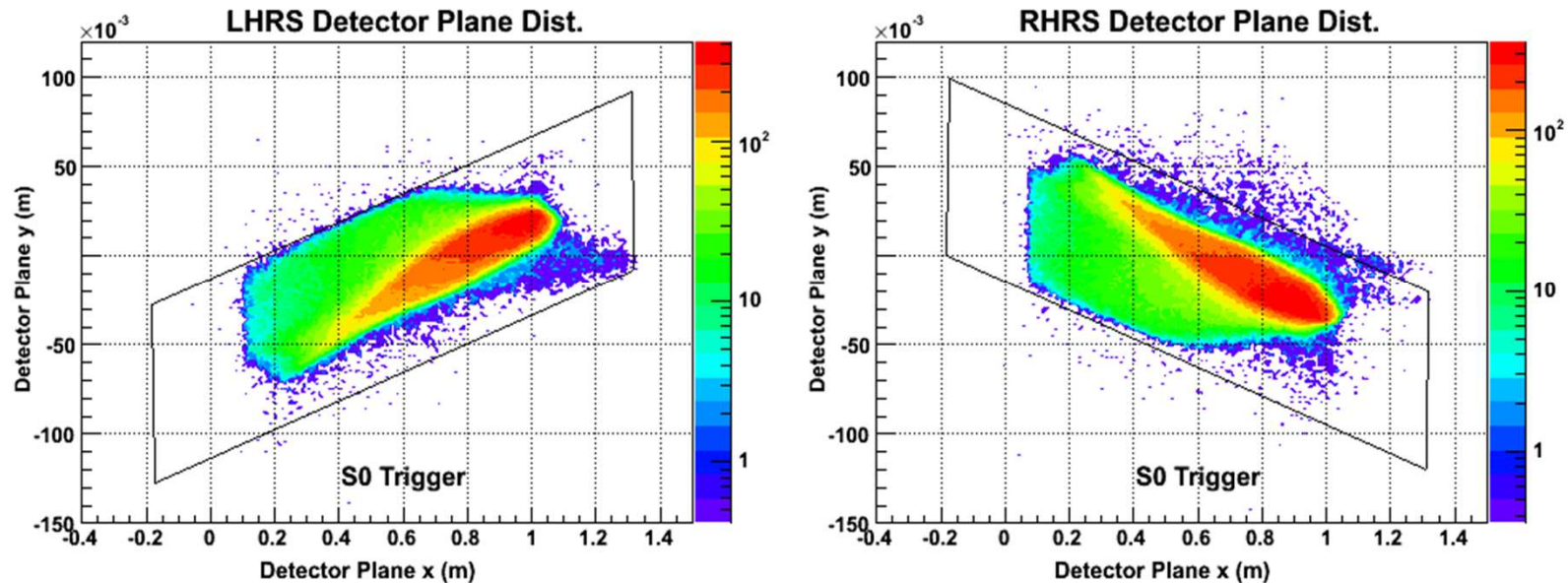


Detectors



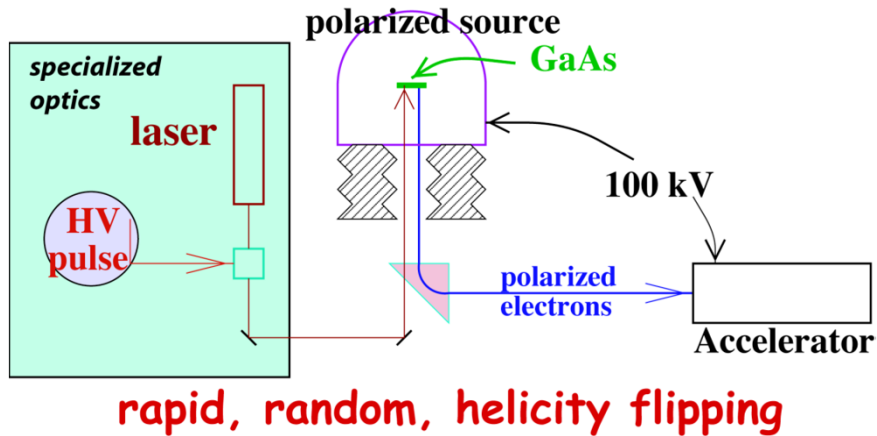
- Lead-Acrylic sandwich calorimeters.
- Cherenkov light from each detector stack is collected by a PMT.
- Doesn't scintillate, so insensitive to soft backgrounds.
- Dimensions chosen to contain the image of elastically scattered electrons, and much of the radiative tail, yet not events from the inelastic scattering.
- Detector orientation adjusted so that the part of the Cherenkov cone is pointed directly at the PMT.

Detector Alignment

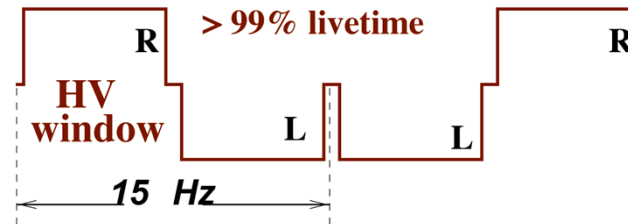


- Entire image of the elastic peak in the focal plane is contained in the detector.
- The inelastics fall outside the detector.

Experimental Method



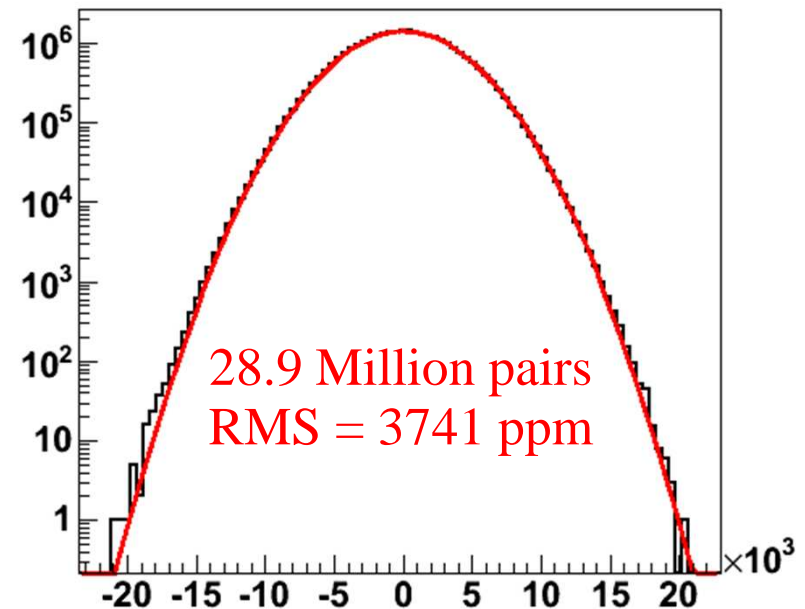
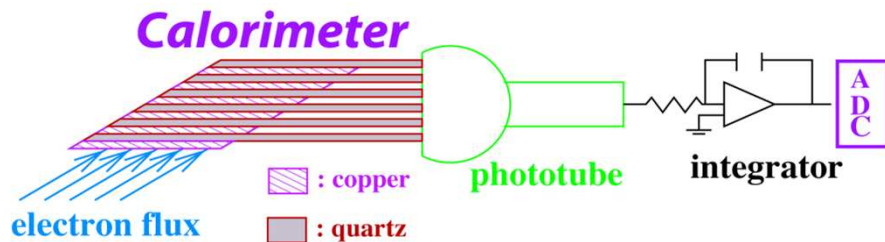
Rapid, Random Helicity Flips



Measure flux F
for each window

$$A_{\text{window pair}} = \frac{F_R - F_L}{F_R + F_L}$$

Flux Integrating Technique HAPPEX = 550 KHz



$$\sigma = \frac{RMS}{\sqrt{N}} = 0.695 \text{ ppm}$$

Measuring Asymmetry

$$A_{mes} = A_{det} - A_{beam} - \sum_i \beta_i \Delta x_i$$

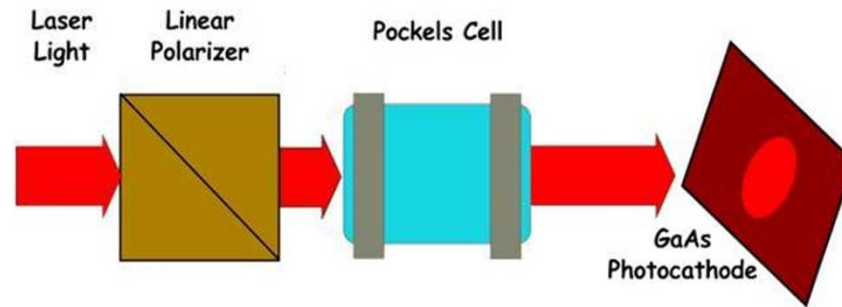
$$A_i = \left(\frac{I_R - IL}{I_R + IL} \right)_i ; \beta_i = \frac{\partial A_{det}}{\partial x_i}$$

A_{det} **includes** A_{beam} (relative window-to-window beam intensity fluctuations) and $\sum_i \beta_i \Delta x_i$ (random beam fluctuations in energy, position and angle)

Left unchecked $\sigma(\text{beam})$ are the dominant source of systematic errors.

HAPPEX III could do without very stringent requirements on the beam, but PREX, which ran after HAPPEX III required very tight control on beam systematics.

Source Setup



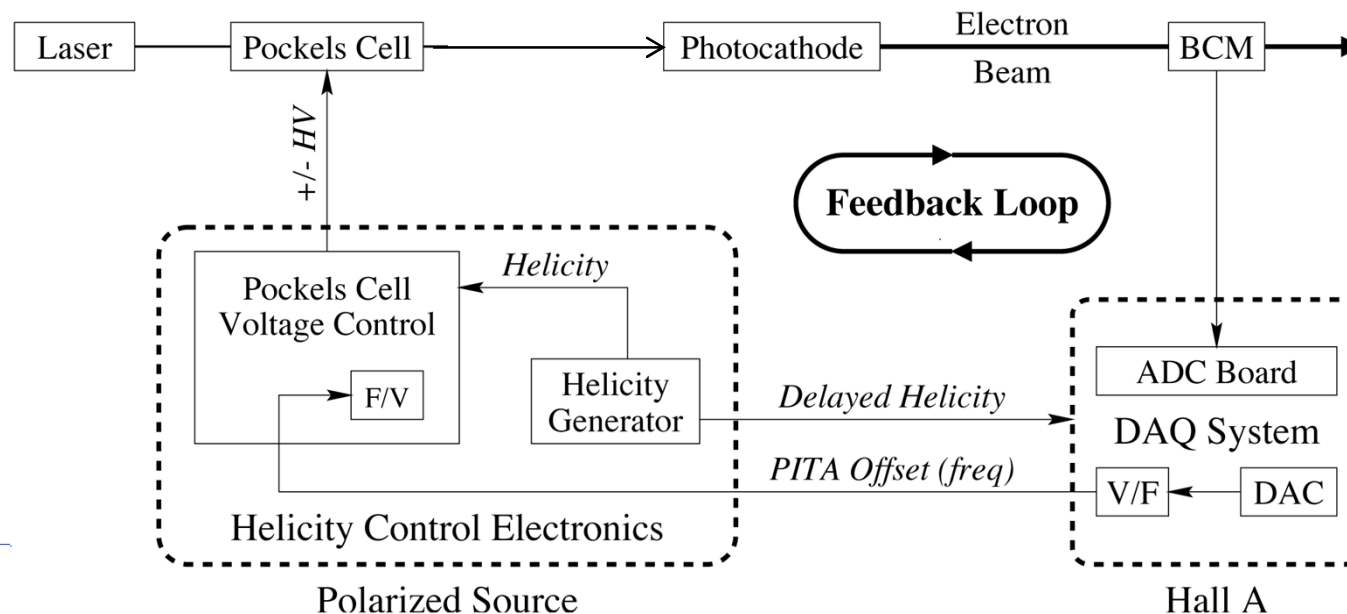
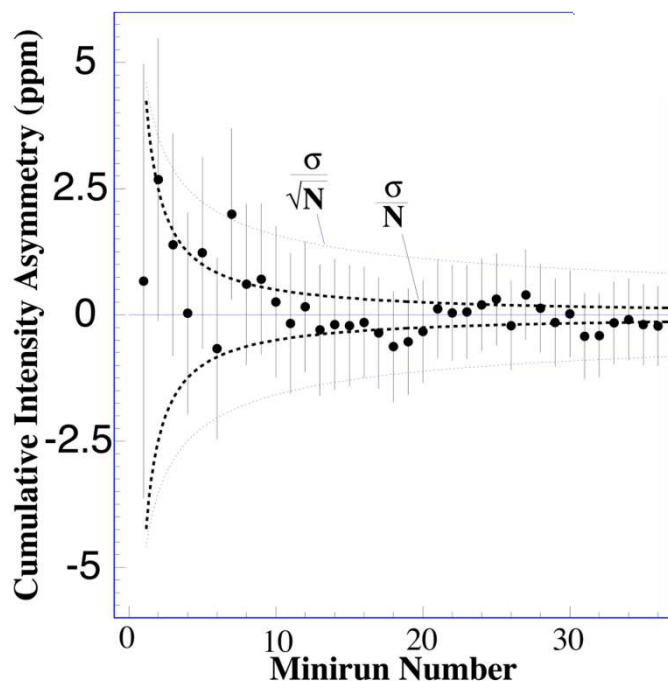
$\pm\lambda/4$ retardation produces
 \pm circular polarization

- The polarized electrons are generated by photoemission from a GaAs photocathode using Right(R)/Left(L) circularly polarized laser beam.
- The electron polarization states are determined by the laser polarization.
- The laser light polarization is prepared using an electro-optic Pockels cell.
 - \pm Quarter-wave phase differences are generated from \pm voltages.
- PC misalignment introduces huge linear residual birefringence on the beam.
- IHPW flips the helicity of the beam (gives us a way of cancelling out the beam systematic effects).

Pockels Cell alignment optimized to minimize A_{beam} & position differences

Intensity Feedback

With passive measures optimized, Feedback zeroes the helicity-correlated effects even further

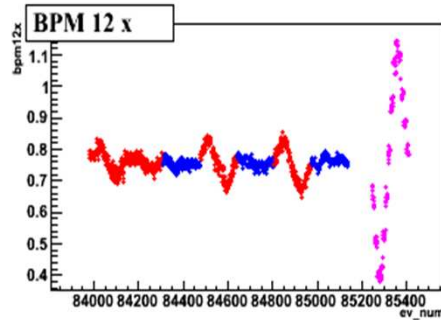
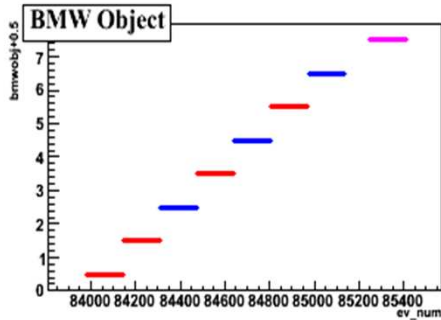


Low jitter and high accuracy allows sub-ppm Cumulative charge asymmetry in ~ 1 hour

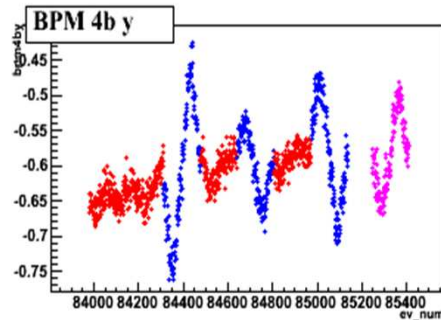
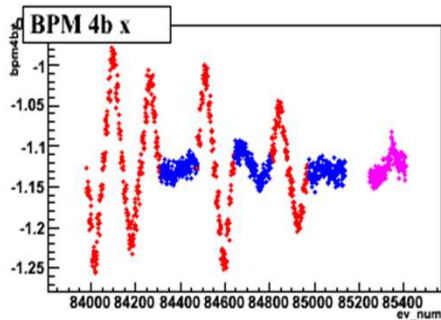
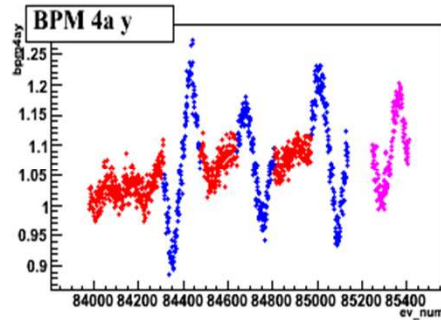
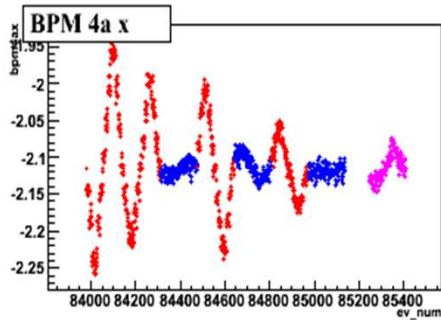
Total charge asymmetry, $A_{\text{beam}} = 202 \text{ ppb}$

Scales as σ/N , not σ/\sqrt{N} as one might naively expect.

Beam Modulation

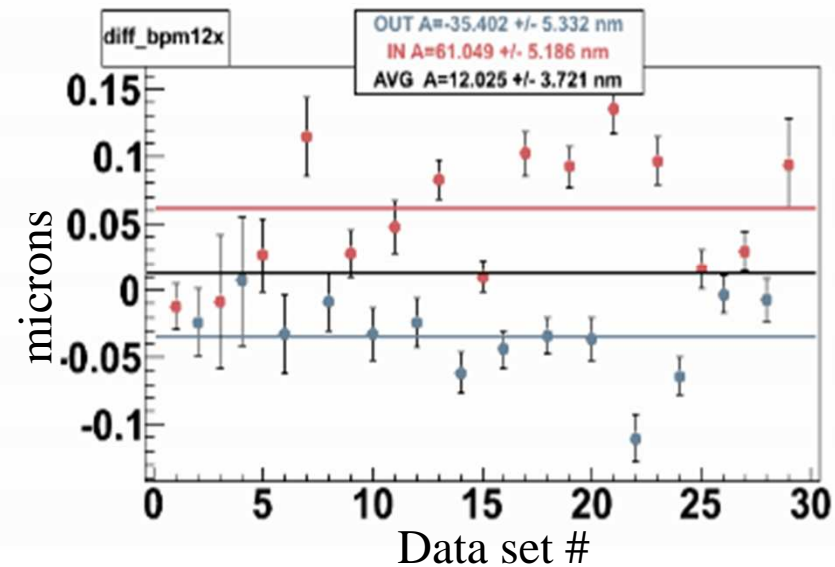
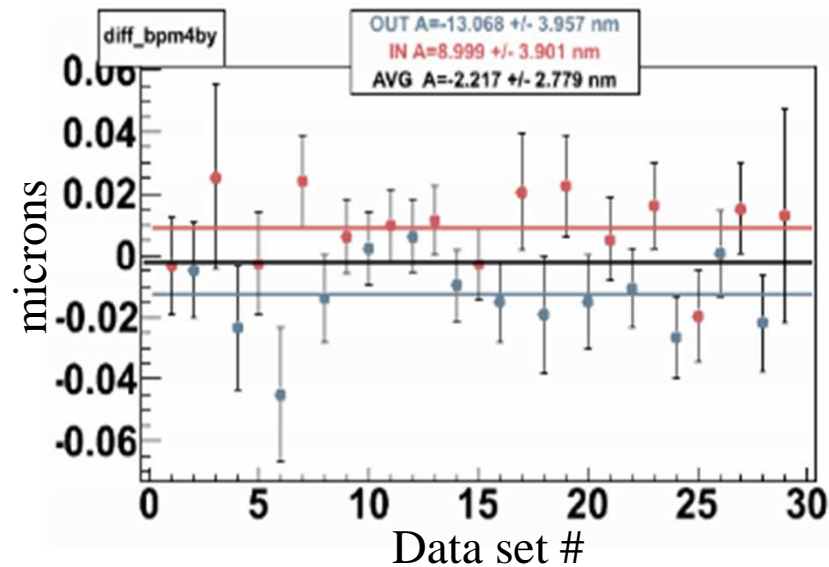


$$\Sigma_i \beta_i \Delta x_i ; \beta_i = \frac{\partial Det}{\partial x_i}$$



- Response of the detectors to these fluctuations can be calibrated by intentionally varying the beam parameters concurrently with data taking.
- Relevant parameters: beam position x and y at the target, angle x and y at the target, and beam energy.
- The energy of the beam is varied by applying a control voltage to a vernier input on a cavity in the accelerator's South Linac.

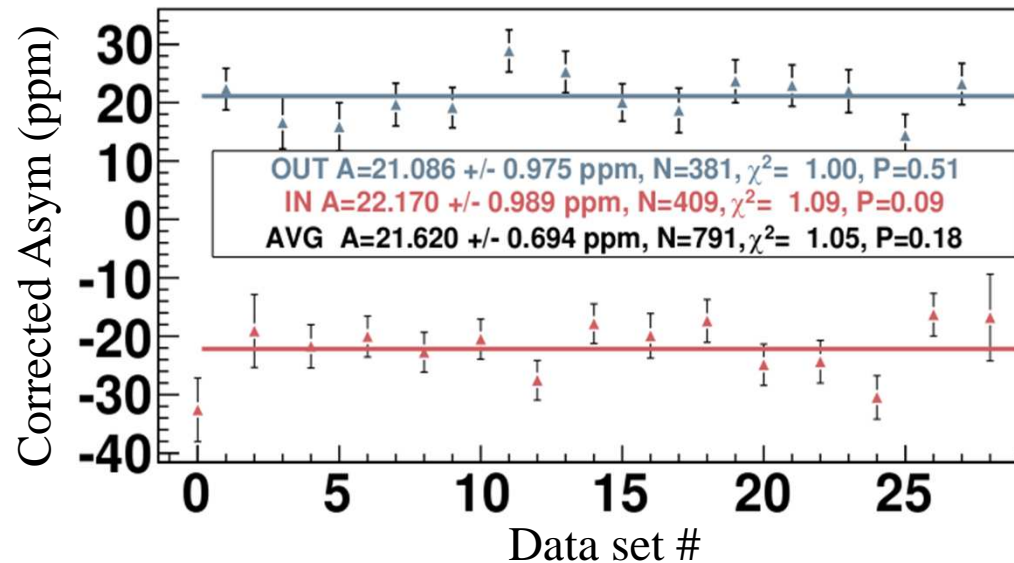
Beam Summary



Energy : 12.0 nm
X position: -2.9 nm
X angle: -0.4 nrad
Y position: -1.8 nm
Y angle: 0.1 nrad

Total Correction = 10 *ppb*.
Total systematic error,
 $\sigma(\text{beam}) = 41 \text{ ppb}$

Measured Asymmetries



$$A_{det} = -21.610 \pm 0.694 \text{ ppm}$$

$$A_{mes} = -21.620 \pm 0.694 \text{ ppm}$$

Corrections are negligible

$$A_{mes} = -21.591 \pm 0.688(stat) \text{ ppm}$$

Systematic Errors

$$\sigma(syst) = \sqrt{(\sigma(\text{beam})^2 + \sigma(K)^2 + \sigma(P_b)^2 + \sigma(\text{backgrounds})^2 + \sigma(Q^2)^2 + \sigma(\text{non-linearities})^2)}$$

$\sigma(\text{beam}) \rightarrow$ *Beam Fluctuations*

$\sigma(K) \rightarrow$ *Kinematic Acceptance*

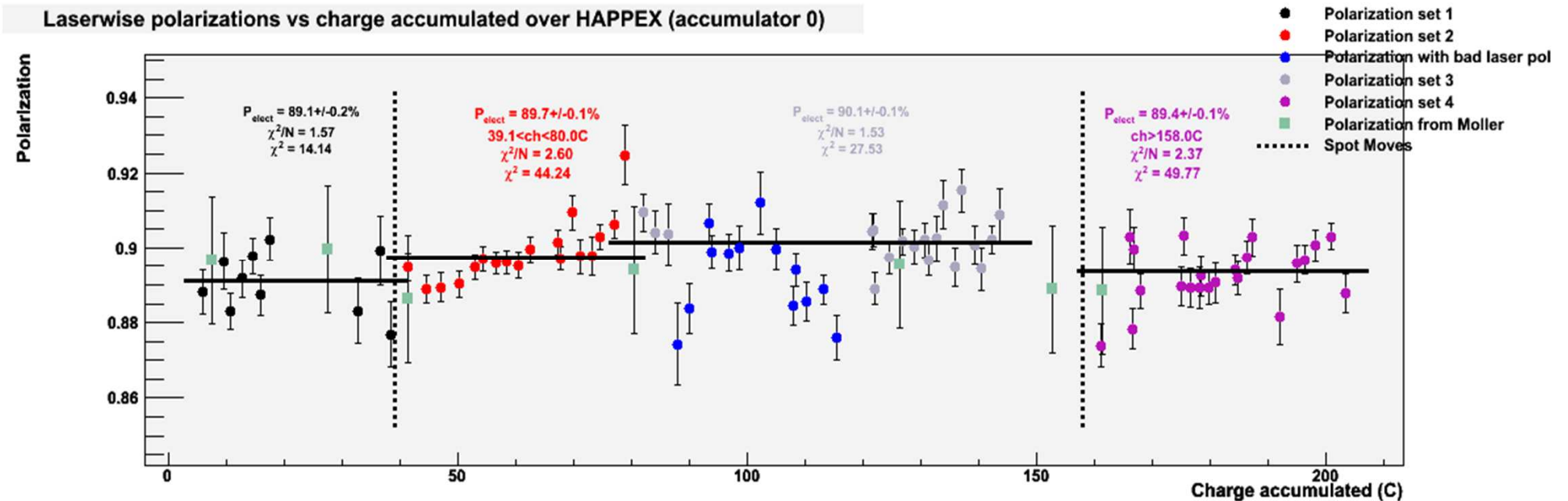
$\sigma(P_b) \rightarrow$ *Beam Polarization*

$\sigma(\text{backgrounds}) \rightarrow$ *Backgrounds*

$\sigma(Q^2) \rightarrow$ *Q^2 Measurement*

$\sigma(\text{non-linearities}) \rightarrow$ *Detector & Monitor non linearities*

Polarization



- Compton: $89.68 \pm 0.95\%$
- Moller: $89.22 \pm 1.7\%$

$$P_b = 89.59 \pm 0.76\%$$

Systematic Error due to P_b , $\sigma(P_b) = 202$ ppb

Backgrounds: Aluminum

- Target Cell is Aluminum. So need to correct for Aluminum background.
- The aluminum backgrounds are dominantly QuasiElastic.
- Al background $\sim 1.0 \pm 0.3$ % on LHRS, $\sim 1.3 \pm 0.4$ % on RHRS.
- Error on Al window thickness measurement ~ 30 %.
- Error on Al asymmetry ~ 30 %.

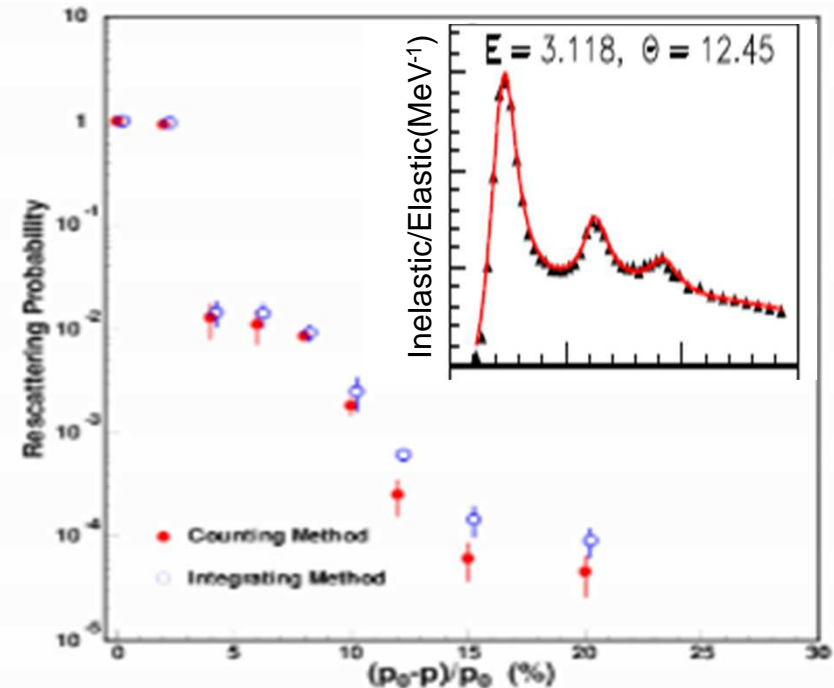
Net Al Background $\sim 1.15 \pm 0.35$ %

Al background correction = 126 ppb
Al background systematic error = 127 ppb

Backgrounds: Inelastic Re-scattering

$$B = \int dE * P(E) * R(E)$$

$$P(E) = \text{rescattering probability};$$
$$R(E) = \sigma_{inel}/\sigma_{el}$$

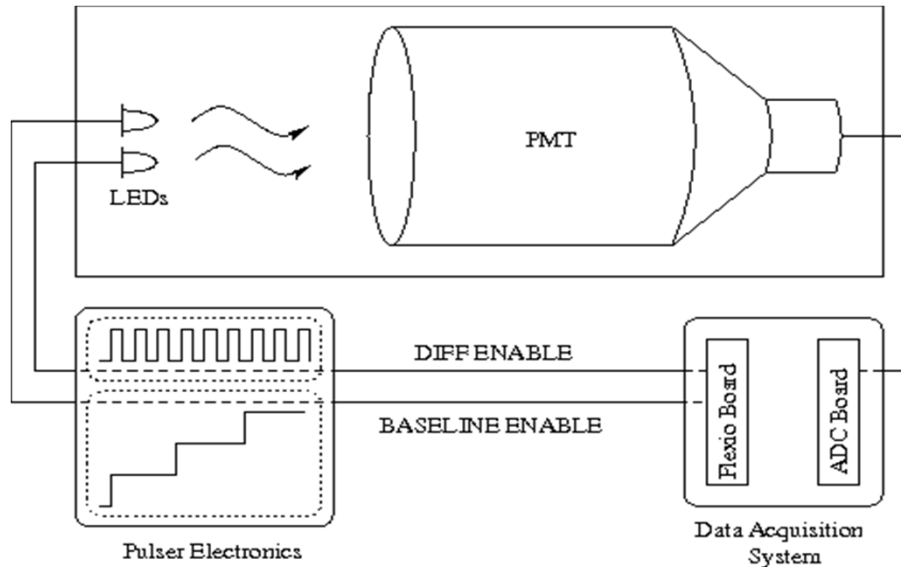


A small fraction of electrons scattered inelastically and re-scattered inside the spectrometer after the dipole also make it to the detector.

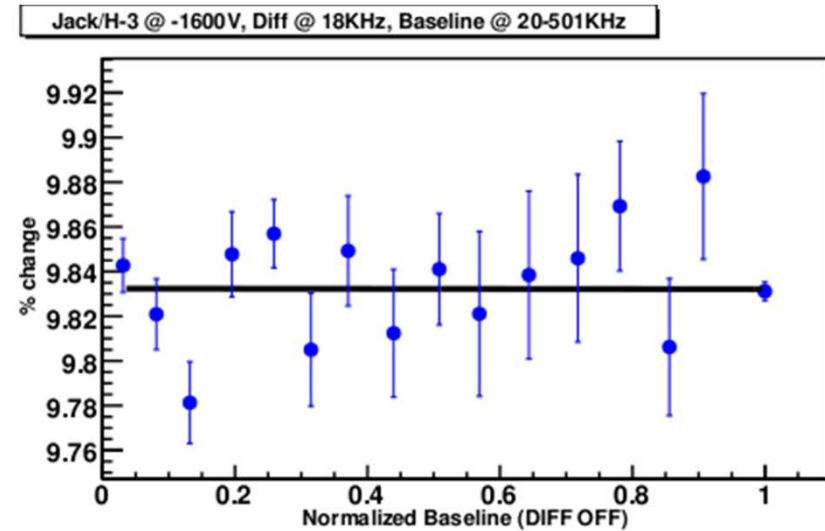
$$\text{Inelastic} = 0.29 \pm 0.075\%$$

Inelastic re-scattering correction = 114 ppb
Inelastic re-scattering systematic error = 55 ppb

Detector Non-Linearity



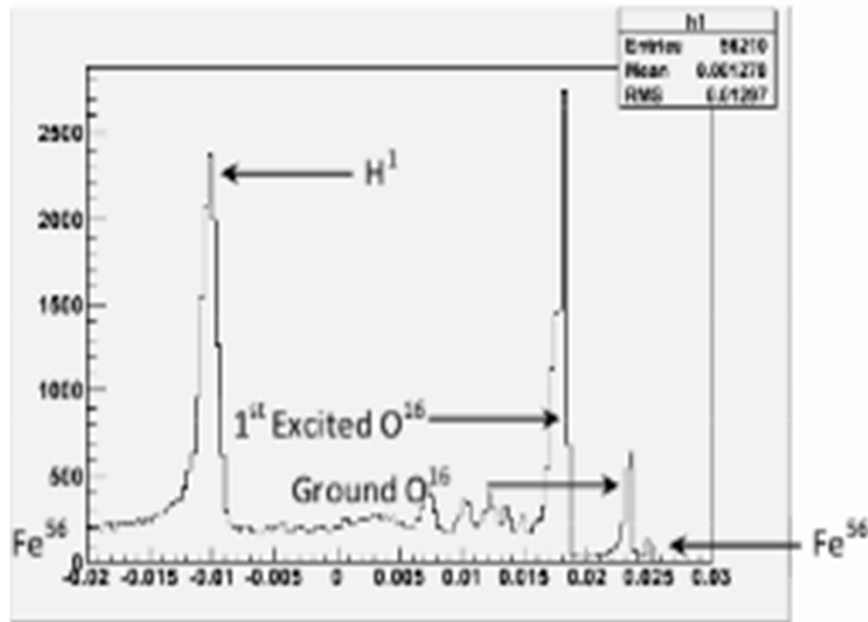
- A pair of blue LEDs is mounted in front of the PMT
- DIFF LED: toggled at a constant freq., toggled ON/OFF.
- BASELINE LED: driven at varying freq. of up to 800 KHz (observed electron rate @ 100 uA)
- The pulses of both LEDs are fixed to be about the size of the electron pulses.



- Non-linearity of the detectors are < 0.1 %.
- A conservative 0.5 % non-linearity is taken as systematic error.

Systematic Error due to detector non-linearity = 129 ppb

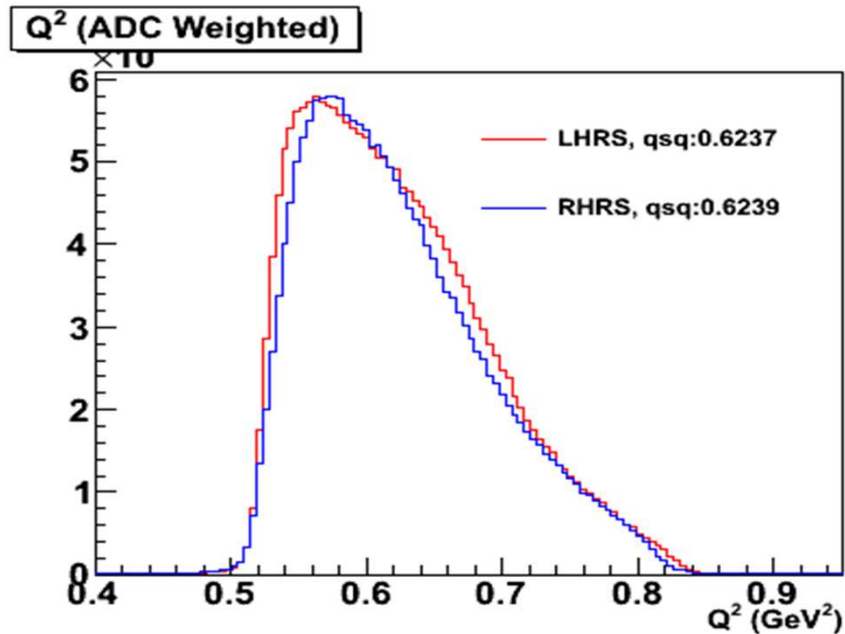
Q² Measurement: Central Scattering Angle



- Dominant error in Q² is from the uncertainty in the central angle measurement.
- Central angle is measured by survey, and pointing study. Survey measurements have larger errors.
- In pointing study, the central scattering angle is determined by measuring energy differences between the ground state oxygen, first excited oxygen, iron and hydrogen elastic peaks from water target runs.
- These energy differences can be measured to about 150 KeV, which for differences of 32-42 MeV is an uncertainty of only 0.45%.

	Hall Center		Target Center		Uncertainty
	LHRS	RHRS	LHRS	RHRS	
Pointing (rad)	0.2463	0.2424	0.2466	0.2389	0.0004
Survey (rad)	0.2443	0.2448	0.2446	0.2413	0.0010

Q^2 Measurement



- Q^2 profile different between the HRS due to differences in acceptances.
- Q^2 varied over the course of the run due to shifts in beam positions.
- 3 distinct LHRS measurements, 4 distinct RHRS measurements.

Error Source	Error	Error in Q^2
Central Angle	0.4 mrad	0.32 %
Beam Energy	3.0 MeV	0.10 %
HRS Momentum	1.5 MeV	0.05 %
Matrix Elements	0.2 mrad	0.16%
Beam Fluctuations	1um	1.4e-3
Drifts in Time		0.2%
ADC Weighting		0.1%
Total		0.44%

$$Q^2 = 0.6421 \pm 0.0028 (\text{GeV}/c)^2$$

Systematic Errors Summary

<u>Error Source</u>	<u>Error</u>	<u>% of Asymmetry</u>
False Asymmetry	41 ppb	0.17 %
<i>Energy (0 ppb)</i>		
<i>Position (34 ppb)</i>		
<i>Charge (23 ppb)</i>		
Polarization	202 ppb	0.85 %
Backgrounds	194 ppb	0.82 %
<i>Aluminum QE (127 ppb)</i>		
<i>Inelastic rescattering (55 ppb)</i>		
<i>Poletip (136 ppb)</i>		
Linearity	129 ppb	0.54 %
<i>Detector linearity (129 ppb)</i>		
<i>BCM linearity (5 ppb)</i>		
Q²	160 ppb	0.67 %
Kinematic Acceptance	48 ppb	0.20 %
Total	353 ppb	1.49 %

Non-strange Asymmetry

$$A_{phys} = AV + As + AA$$

$$A_V = -A_0 \left[(1 - 4 \sin^2 \theta) - \frac{\epsilon G p E G^n_E + \tau G p M G n_M}{\epsilon (G^p_E)^2 + \tau (G^p_M)^2} \right]$$

$$A_s = A_0 \frac{\epsilon G p E G^s_E + \tau G p M G s_M}{\epsilon (G^p_E)^2 + \tau (G^p_M)^2}$$

$$A_A = A_0 \frac{(1 - 4 \sin^2 \theta) \epsilon' G^p_M \tilde{G}^p_A}{\epsilon (G^p_E)^2 + \tau (G^p_M)^2}$$

Contains higher order corrections

$$A_{NVS} = AV + AA = -24.060 \pm 0.734(FF) \text{ ppm}$$

Form Factors

$$A_{mes} = -21.591 \pm 0.688(stat) ppm$$

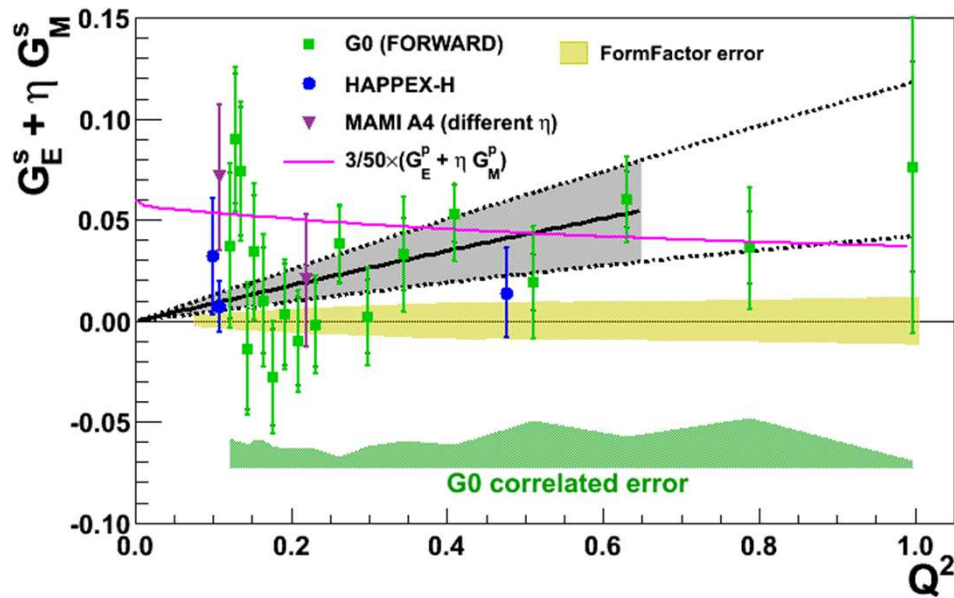
$$A_{phys} = \frac{K}{P_b} (A_{mes} - Pb \sum_i f_i A_i) / (1 - \sum_i f_i)$$

$$A_{phys} = -23.742 \pm 0.776(stat) \pm 0.353(syst) ppm$$

$$@ Q^2 = 0.6421 \pm 0.0028 (GeV/c)^2$$

$$G^s_E + 0.517 G^s_M = 0.004 \pm 0.010(stat) + 0.004(syst) + 0.009(FF)$$

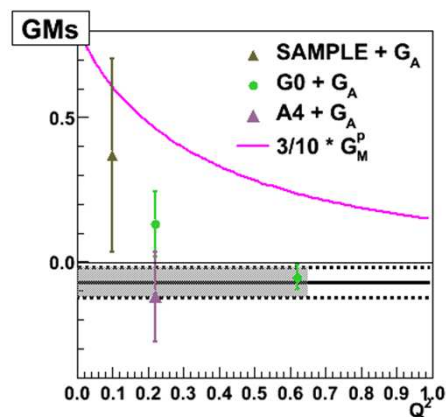
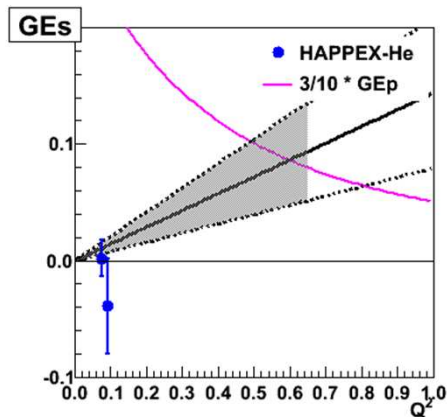
Form Factors (H3 excluded)



Fit to “leading order” in Q^2 ,
(only for $Q^2 < 0.65 \text{ GeV}^2$)

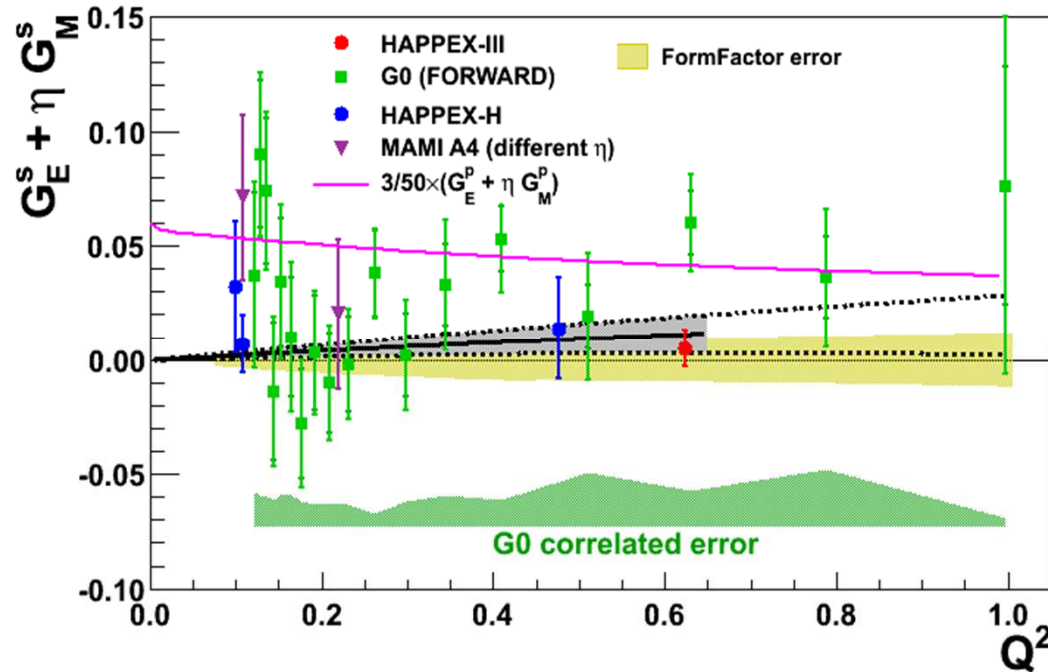
$$G_M^s = \mu_s$$

$$G_E^s = \rho_s * \tau$$

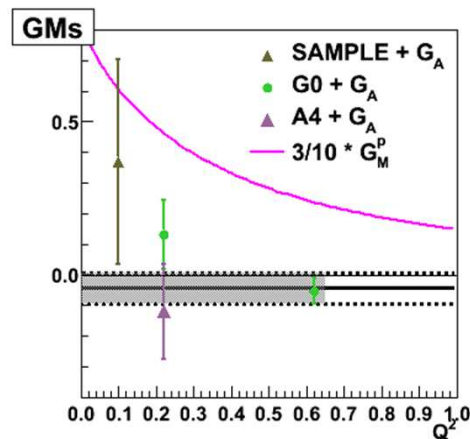
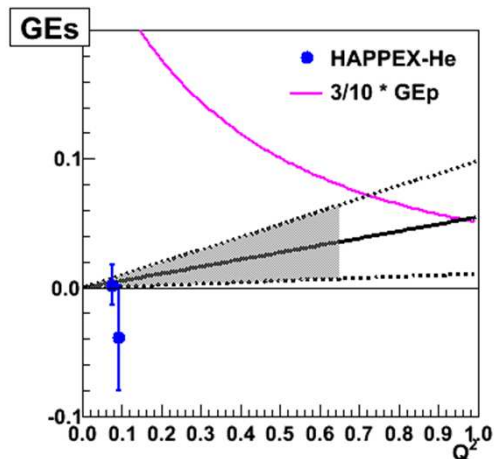


G_M^s From backangle
results, neglects
correlation with G_E^s

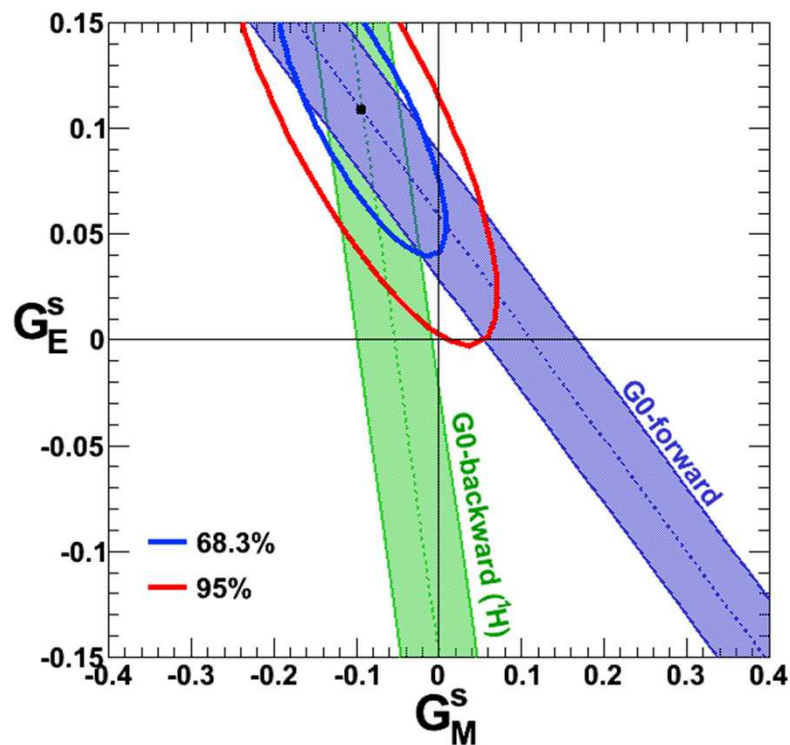
Form Factors



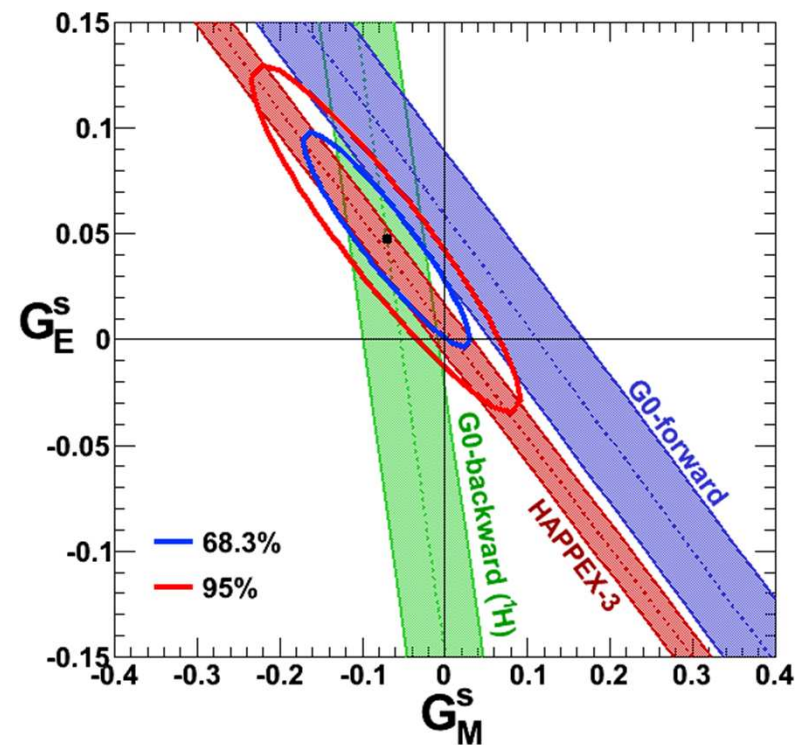
- $Q^2 < 0.65$ fit is much closer to 0.
- All HAPPEX data consistently point to 0 strangeness contribution to form factors.



World Data @ $Q^2=0.6 \text{ (GeV/c)}^2$



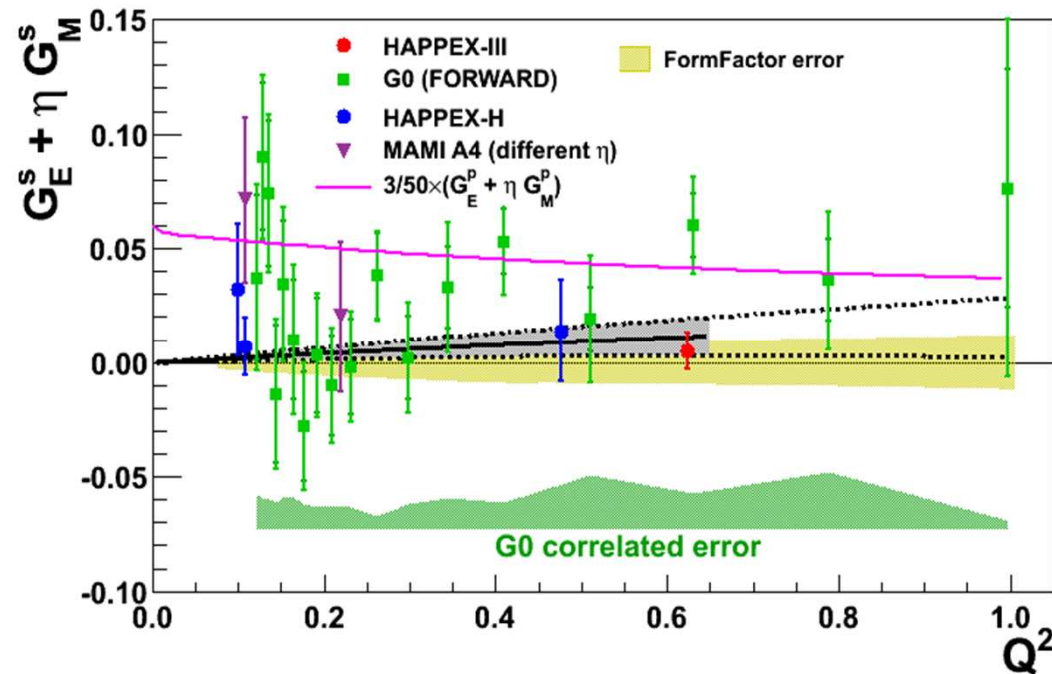
H3 data not included



H3 data included

- Although the data does lean a little positive, not very pronounced statistically.
- HAPPEX III, and the rest of HAPPEX results, which are the most precise measurements of the strange form factors, are all consistently zero.

Conclusions



- HAPPEX III measured a strange form factor of 0, within the uncertainty.
- Recent lattice QCD results suggest a non-zero strange form factor, but with values smaller than the current FF uncertainties.
- Further improvements in precision would require additional theoretical improvements.

Acknowledgements

Dr. Kent Paschke

Dr. Gordon Cates

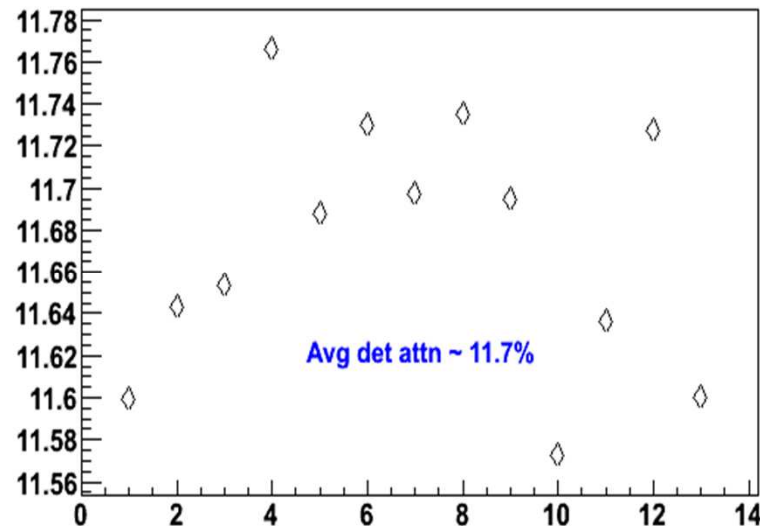
HAPPEX III Collaboration

Questions??

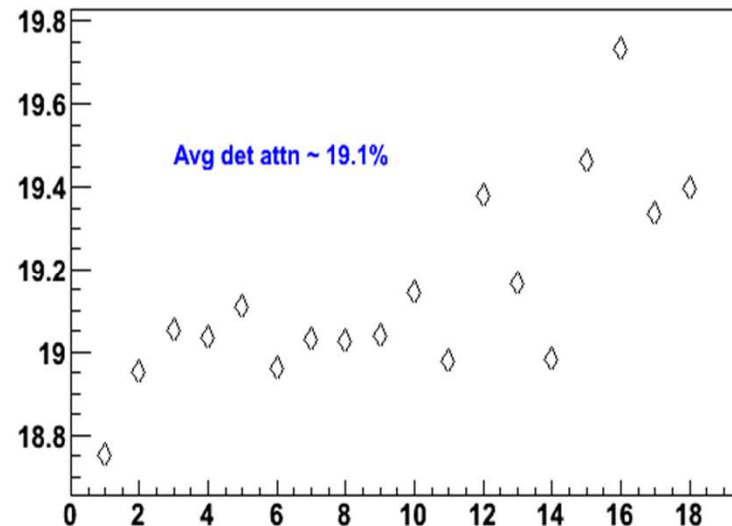
EXTRA SLIDES

Detector Efficiency

Det Atten Coeff LHRS (% per m)

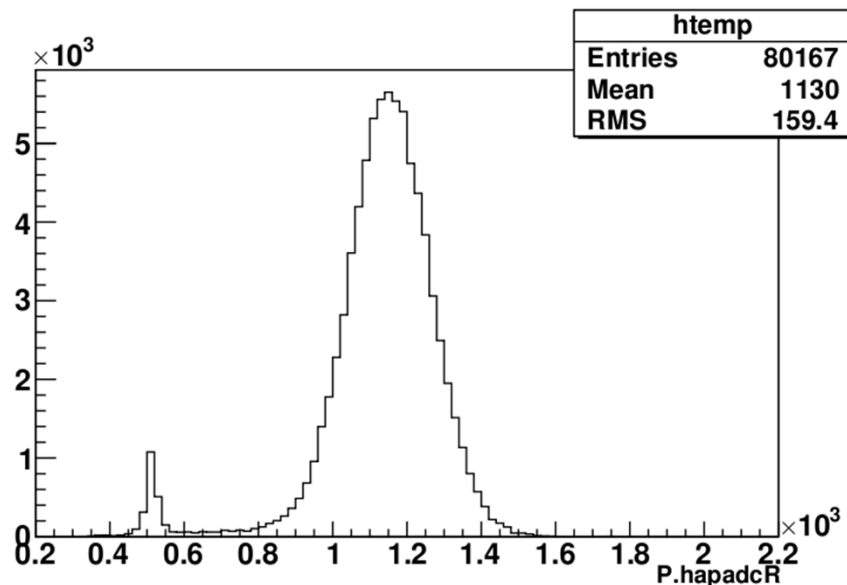


Det Atten Coeff RHRS (% per m)



- Signal output is a strong function of the particle's position along the detector's length.
- Characterizing this dependence is important for calibrating asymmetry measurements.
- Installed a single sheet of Plexiglass directly in front of the PMT to filter out UV radiation. (50%/m decrease in light output without the Plexiglass.)
- Plexiglass reduced the total signal size, but the dependence of light output along the detector decreased to about 11.7%/m on the LHRS detector and 19.1%/m on the RHRS detector.
- Look at the detector attenuation to check that the detectors did not deteriorate over the course of the run.

Detector Energy Resolution



$$R = \sigma_{\text{det}} / \text{mean}_{\text{det}}$$

The detector energy resolution increases the statistical error by a factor $\sqrt{(1+R^2)}$.

- LHRS detector energy resolution is 8.13%, which increases the statistical error by $\sim 0.3\%$.
- RHRS detector energy resolution is 14.1%, which increases the statistical error by $\sim 1.0\%$.

Transverse Asymmetry

Transverse asymmetry: -10 ppm +/- 5 ppm.

** Estimated horizontal polarization during run: 0.0% +/- 10% **

- acceptance around horizontal: factor of 20%

- acceptance symmetry: factor of 10%

Potential systematic error:

$10\text{ppm} * 20\% * 10\% * 10\%$ (horizontal polarization): = 0.02 ppm

(correction = 0)

** Estimated vertical polarization during run: 0.0% +/- 2% **

The left/right arms were nearly perfectly matched in Q2, and

matched in rate/precision as well. They are weighted the

same. There is no nominal first order correction, but we

could conservatively consider the second order terms $dP_v * dA$

and $dP_v * dW_t * \sigma_A$ (but the weights are equal, so $dW_t = 0$ and

we have only one term):

assume transverse is linear in Q2, consider systematic error in Q2 as independent on each arm:

$$(dQ^2 / Q2) * A * dP_v = 0.4\% * 10\text{ppm} * 2\% = 0.0008 \text{ ppm}$$

Backgrounds: Poletip

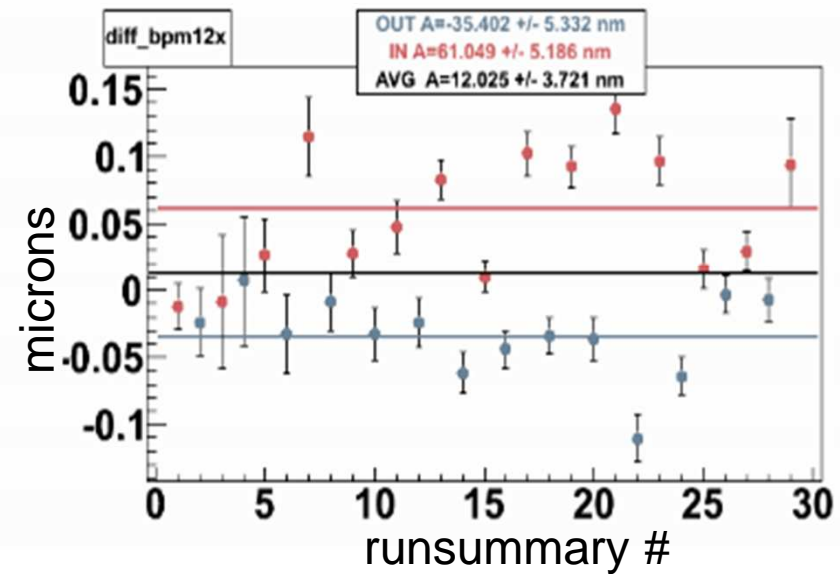
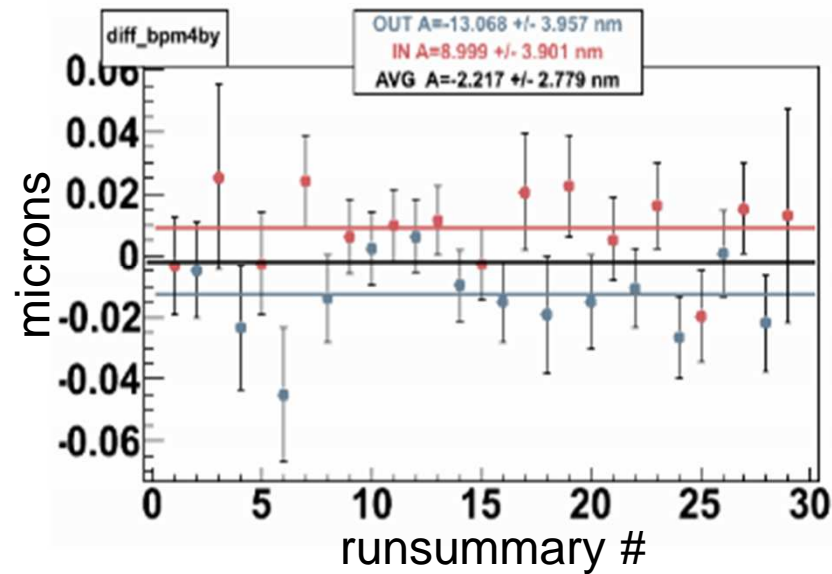
Scattering from the magnetized iron in the spectrometer is a potential source of systematic error.

$$dA = f P_{e1} P_{e2} A$$

f is the fractional signal size ($f \ll 10^{-4}$), P_{e1} , P_{e2} are the polarizations of the scattered electron and the electron in iron ($P_{e1} \sim 0.8$, $P_{e2} \sim 0.03$) and A is the analyzing power ($A \leq 0.11$).

Poletip correction = 0 ppb
Poletip systematic error = 136 ppb

Beam Summary



	bcm1(ppm)	bpm4ax(nm)	bpm4ay(nm)	bpm4bx(nm)	bpm4by(nm)	bpm12x(nm)
IHWP OUT	-0.37 ± 0.22	-6.0 ± 3.2	-13.0 ± 4.2	-2.2 ± 3.3	-13.1 ± 4.0	-35.4 ± 5.3
IHWP IN	-0.03 ± 0.22	0.3 ± 3.5	9.8 ± 4.2	0.9 ± 3.6	9.0 ± 3.9	61.0 ± 5.2
IHWP BOTH	-0.20 ± 0.16	-2.9 ± 2.4	-1.8 ± 3.0	-0.7 ± 2.4	-2.2 ± 2.8	12.0 ± 3.7

Measured Asymmetries

IHWP = OUT							
	Raw(0-28)	Cor(0-28)	Reg(0-28)	Reg(0-2)	Dit(3-28)	Raw-Cor	Raw-Reg
det1	21.650 ± 1.352	21.686 ± 1.352	21.664 ± 1.351	21.462 ± 4.919	21.704 ± 1.406	-0.036	-0.014
det2	20.535 ± 1.349	20.554 ± 1.349	20.581 ± 1.349	23.188 ± 4.933	20.341 ± 1.403	-0.019	-0.046
det_all	21.060 ± 0.975	21.086 ± 0.975	21.089 ± 0.974	22.303 ± 3.556	20.987 ± 1.013	-0.026	-0.030
det1-det2	1.104 ± 1.910	1.120 ± 1.910	1.071 ± 1.909	-1.909 ± 6.967	1.367 ± 1.986	-0.017	0.032
IHWP = IN							
	Raw(0-28)	Cor(0-28)	Reg(0-28)	Reg(0-2)	Dit(3-28)	Raw-Cor	Raw-Reg
det1	23.049 ± 1.374	23.061 ± 1.374	23.074 ± 1.373	31.353 ± 5.681	22.546 ± 1.416	-0.012	-0.024
det2	21.284 ± 1.372	21.257 ± 1.372	21.239 ± 1.371	22.042 ± 5.749	21.210 ± 1.413	0.027	0.045
det_all	22.177 ± 0.989	22.170 ± 0.989	22.167 ± 0.989	26.773 ± 4.103	21.886 ± 1.019	0.007	0.009
det1-det2	1.749 ± 1.942	1.788 ± 1.942	1.818 ± 1.941	9.124 ± 8.083	1.339 ± 2.000	-0.039	-0.069
IHWP = ALL							
	Raw(0-28)	Cor(0-28)	Reg(0-28)	Reg(0-2)	Dit(3-28)	Raw-Cor	Raw-Reg
det1	22.338 ± 0.964	22.362 ± 0.964	22.357 ± 0.963	25.700 ± 3.719	22.122 ± 0.998	-0.024	-0.019
det2	20.903 ± 0.962	20.900 ± 0.962	20.904 ± 0.961	22.702 ± 3.743	20.772 ± 0.995	0.004	-0.001
det_all	21.610 ± 0.694	21.620 ± 0.694	21.620 ± 0.694	24.221 ± 2.687	21.434 ± 0.719	-0.010	-0.011
det1-det2	1.421 ± 1.362	1.449 ± 1.362	1.438 ± 1.361	2.794 ± 5.277	1.353 ± 1.409	-0.028	-0.018

$A_m(\text{Both HRS})$	-21.620 +/- 0.694
$A_m(\text{Left HRS})$	-21.697 +/- 7.406
$A_m(\text{Right HRS})$	-17.621 +/- 8.000

$$A_{\text{mes}}(\text{total}) = -21.591 \pm 0.688 \text{ ppm}$$

Measuring beam jitter sensitivity

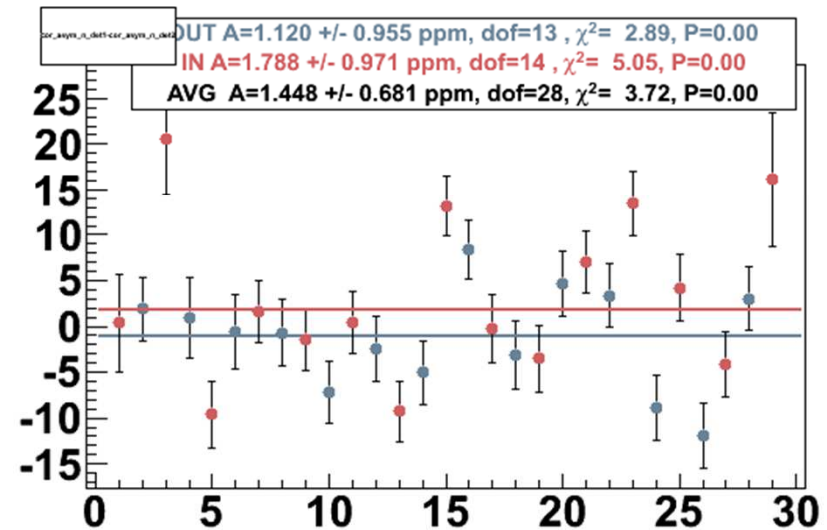
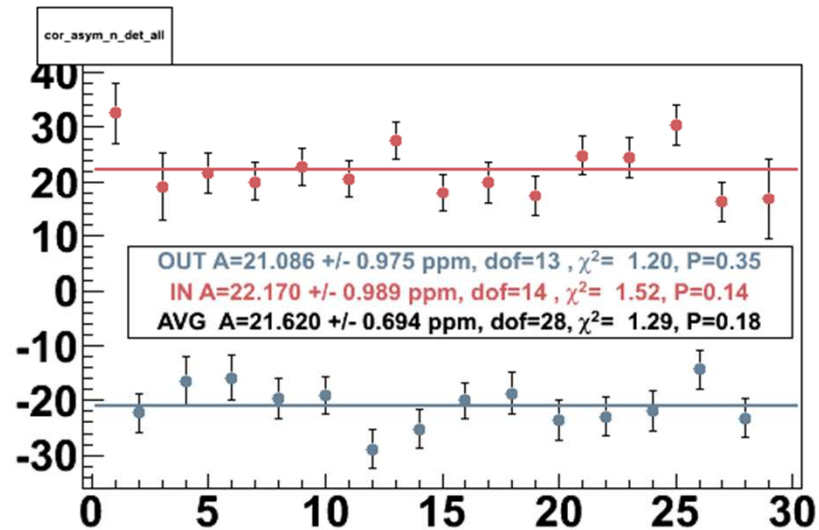
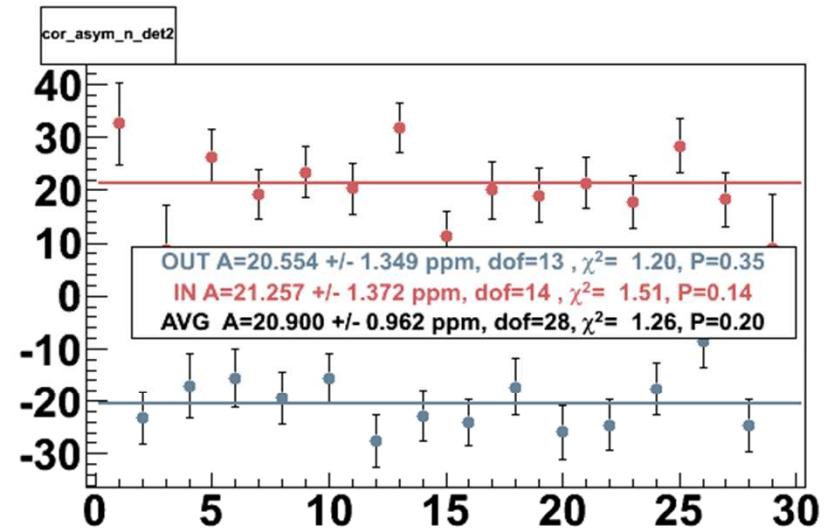
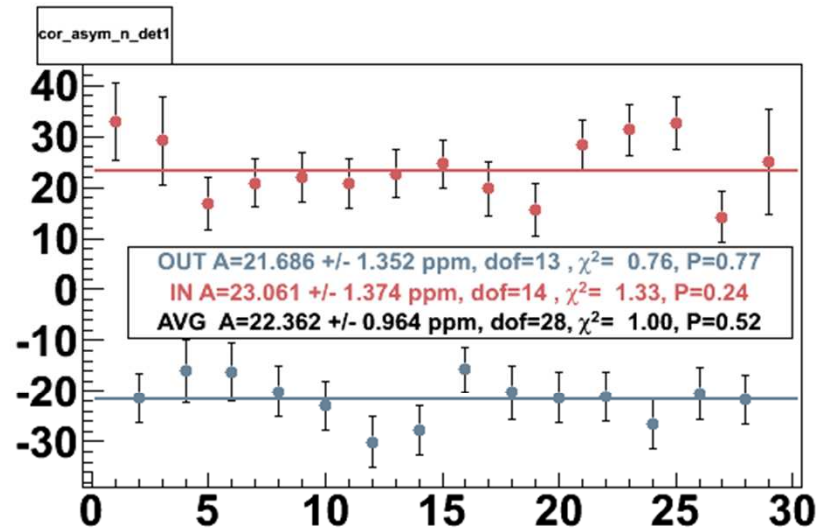
The beam jitters and HC position differences generate false asymmetries, and increase the statistical width of measurements.

Two independent methods are used to correct the false asymmetries due to beam HC position differences, and remove the effects of beam jitter.

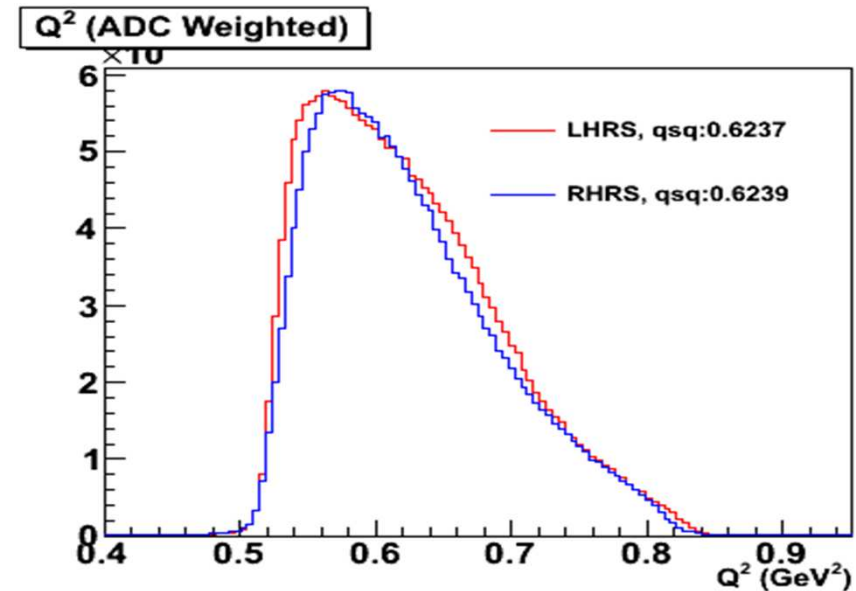
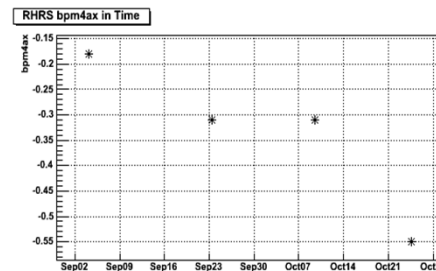
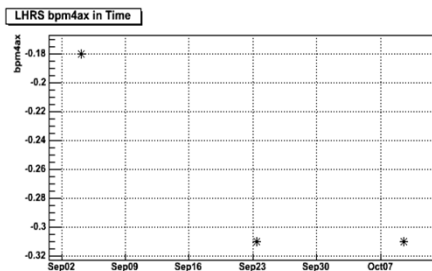
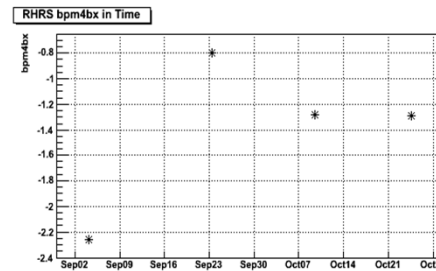
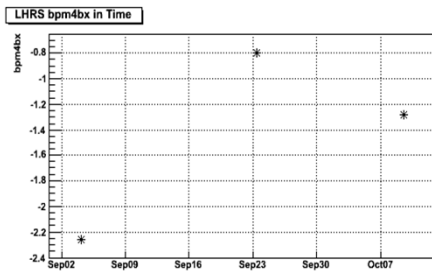
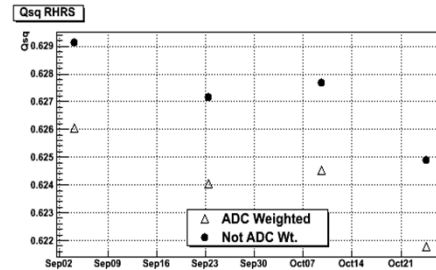
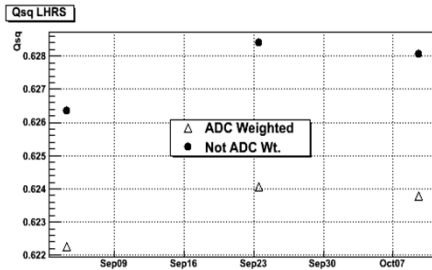
- Beam Modulation: Response of the detectors to these fluctuations can be calibrated by intentionally varying the beam parameters concurrently with data taking.
- Regression: Natural motion of the beam is used to regress out the false asymmetries due to position differences. Slopes are determined by via least-squares algorithm.

$$A_{mes} = A_{det} + \sum_i \beta_i \Delta x_i$$

Measured Asymmetries



Q^2 Measurement



- Q^2 profile different between the HRS due to differences in acceptances.
- Q^2 varied over the course of the run due to shifts in beam positions.
- 3 distinct LHRS measurements, 4 distinct RHRS measurements.

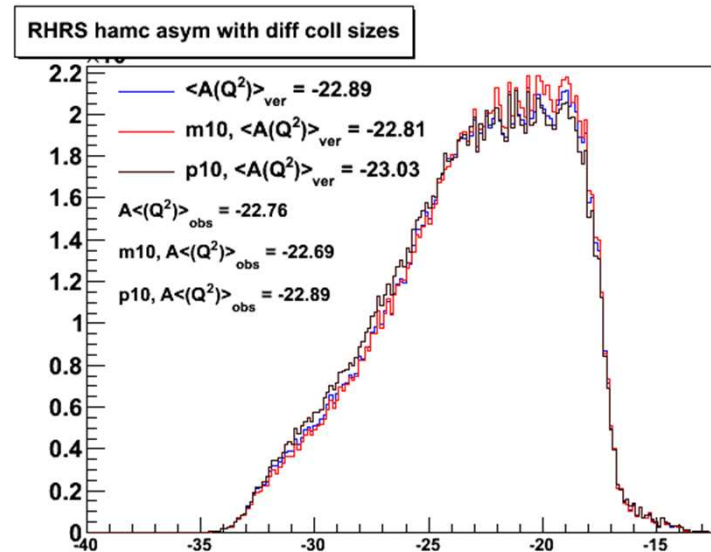
	Q^2 (GeV/c) ²
LHRS	0.6239
RHRS	0.6243
Average	0.6241

Q^2 Systematic Errors

<u>Error Source</u>	<u>Error</u>	<u>Error in Q^2</u>
Central Angle	0.4 mrad	0.32 %
HRS momentum	1.5 MeV	0.05 %
Beam Energy	3.0 MeV	0.10 %
Matrix Elements	0.2 mrad	0.16 %
Beam Position Fluctuations	1 μ m	1.4e-3 %
Drifts in Time		0.2 %
ADC Weighting		0.1 %
Total		0.44 %

$$Q^2 = 0.6421 \pm 0.0028 \text{ (GeV/c)}^2$$

Kinematic Acceptance



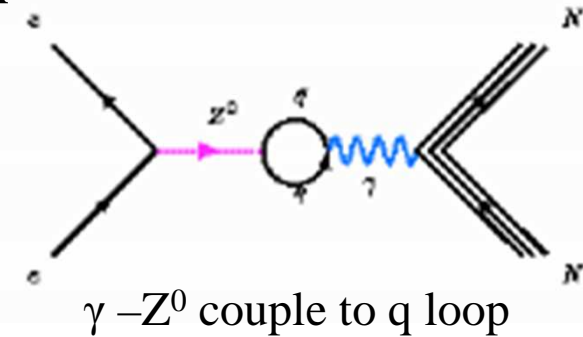
- The measured asymmetry is a convolution over a range of Q^2 due to finite acceptance of the spectrometer, and radiative energy losses.
- The acceptance averaged asymmetry is needs to be corrected to get a point scattering kinematics.

$$K = \frac{A \langle Q^2_{obs} \rangle}{\langle A(Q^2_{ver}) \rangle} = 0.995$$

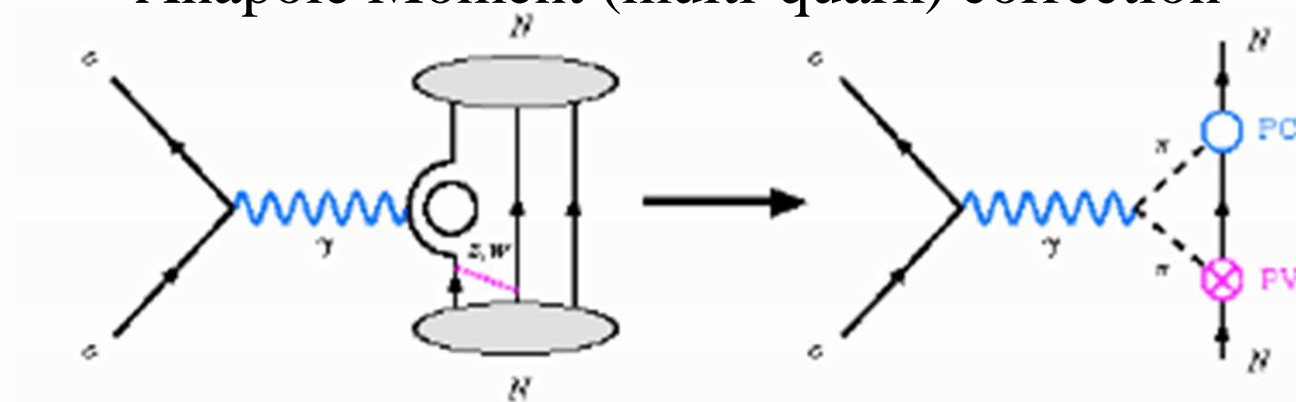
Higher-Order Corrections

One-Quark correction

- Electroweak radiative corrections
- Calculable in Standard Model with little theoretical uncertainty



Anapole Moment (multi-quark) correction



Parity Violating pion emission followed by a Parity Conserving pion emission through the strong interaction.

- Purely Weak Interactions among the quarks in the nucleon.
- Large amount of theoretical uncertainty due to the impossibility of inclusion of all the virtual hadronic states in the calculations.

Measuring Asymmetry

$$A_{mes} = A_{det} - A_{beam} - \sum_i \beta_i \Delta x_i$$

$$A_i = \left(\frac{I_R - IL}{I_R + IL} \right)_i ; \beta_i = \frac{\partial A_{det}}{\partial x_i}$$

A_{det} **includes** A_{beam} (relative window-to-window beam intensity fluctuations) and $\sum_i \beta_i \Delta x_i$ (random beam fluctuations in energy, position and angle)

$$\sigma(A_{mes})^2 = \sigma(statistical)^2 + \sigma(systematic)^2$$

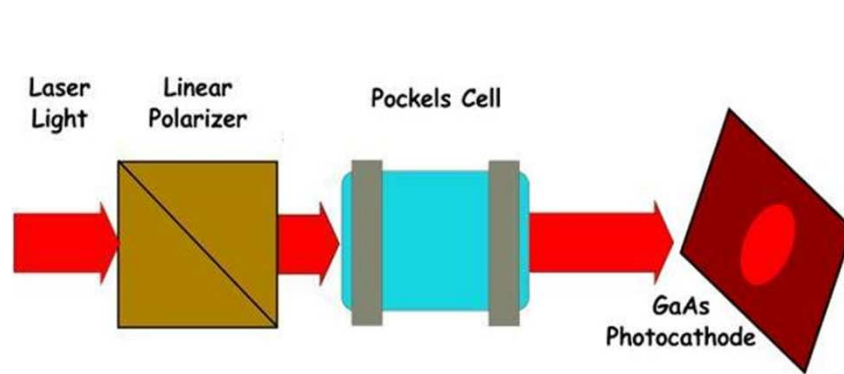
$$\sigma(statistical)^2 \rightarrow \sigma(A_{det})^2$$

$$\sigma(systematic)^2 \rightarrow \sigma(beam)^2 + \dots$$

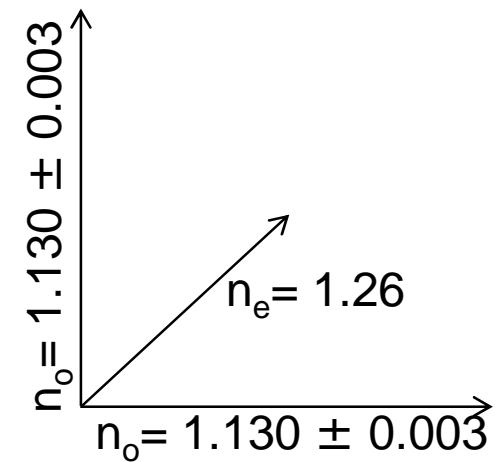
Left unchecked $\sigma(beam)$ are the dominant source of systematic errors.

HAPPEX III could do without very stringent requirements on the beam, but PREX, which ran after HAPPEX III required very tight control on beam systematics.

Source Setup



$\pm\lambda/4$ retardation produces
 \pm circular polarization



- The polarized electrons are generated by photoemission from a GaAs photocathode using Right(R)/Left(L) circularly polarized laser beam.
- The electron polarization states are determined by the laser polarization.
- The laser light polarization is prepared using an electro-optic Pockels cell.
 - \pm Quarter-wave phase differences are generated from \pm voltages.

PC misalignment introduces huge linear residual birefringence on the beam, and increases sensitivity to any voltage fluctuations

Pockels Cell alignment optimized to minimize A_{beam} & position differences